Structure of the Deoxytetranucleotide d-pApTpApT and a Sequence-Dependent Model for Poly(dA-dT)*

M. A. VISWAMITRA, *Department of Physics, Indian Institute of Science, Bangalore 560012, India;* ZIPPORA SHAKKED, *Department of Structural Chemistry, The Weizmann Institute of Science, Rehovot, Israel;* and P. G. JONES, G. M. SHELDRICK, S. A. SALISBURY, and OLGA KENNARD, *University Chemical Laboratory, Lensfield Road, Cambridge, United Kingdom*

Synopsis

The x-ray structure of the hydrated ammonium salt of the deoxytetranucleotide d-pApTpApT was determined by Patterson and direct methods at a resolution of 1 Å. The crystal structure contains right-handed double-helical segments formed by complementary Watson-Crick-type hydrogen bonding between the adenine and thymine bases of neighboring molecules. The minihelix contains two base pairs. The chains are antiparallel. The A-T and T-A sequences have different phosphodiester conformations. The deoxyribose-pucker and the sugar–base orientation alternate along the chain depending on the nature of the base (3′-*endo* for purine and 2′-*endo* for pyrimidine). The extended structure is stabilized by base–base, base–sugar, and hydrogen-bond interactions. The minihelix of two base pairs provides starting coordinates for model-building studies of the dA-dT polymer. A B-DNA-type polymer structure is described, which has sequence-dependent alternations of both the deoxyribose pucker and the phosphate diester bridge conformation. Such sequence-dependent DNA structures, if present locally in regions such as operator sequences, could facilitate sequence-specific interactions. The crystal study also suggests possible geometrical parameters for the replication fork.

INTRODUCTION

Since the discovery of the DNA double helix by Watson and Crick,[1] a large body of physicochemical and biological information has accumulated on the structure of the genetic material. Many details of different helical structures of DNA and the influence of environmental factors such as hydration and the presence of metal ions, as well as the dependence of the DNA secondary structure on base composition and sequence, have been obtained mainly from analyses of x-ray fiber-diffraction patterns.[2]

Much of today's thinking is directed at an understanding of how the nucleotide sequences of the double helix are selectively recognized by proteins. This requires a knowledge of the way in which specific base pairs

* Supplementary material on observed and calculated structure factors for d-pApTpApT is available from the authors.

Biopolymers, Vol. 21, 513–533 (1982)

CCC 0006-3525/82/030513-21$02.10

and base sequences affect the finer details of the DNA structure. Such information cannot be obtained by the methods mentioned above, since the limited data they provide can only be used to visualize an overall averaged structure of the nucleic acid. Geometrical information about the detailed characteristics of the DNA double helix has only recently been obtained from the single-crystal analyses of the tetranucleotide d(pApTpApT),[3] the hexanucleotide d(CpGpCpGpCpG),[4] and of the tetranucleotide d(CpGpCpG).[5,6] d(pApTpApT)[3] provided, for the first time, geometrical details at atomic resolution on right-handed double-helical fragments of DNA of the B-type. It also suggested a sequence-dependent alternating B-DNA-type structure for poly(dA-dT). The other oligonucleotides showed left-handed double-helical structures with a zigzag backbone.

A more recent work is concerned with the crystal structure analysis of d(CpGpCpGpApApTpTpCpGpCpG)[7] at 1.9-Å resolution, which presents a complete turn of B-DNA.

This paper describes the detailed crystal and molecular structures of the oligodeoxynucleotide 5′-P-adenylyl-3′,5′-thymidylyl-3′,5′-adenylyl-3′,5′-thymidine d(pApTpApT) (Fig. 1) based on an x-ray analysis of its ammonium salt. A double-helical fragment consisting of two base pairs found in the crystal structure was used as a starting point in computer model-building studies to generate a B-DNA-type (dA-dT) polymer having a sequence-dependent sugar–phosphate backbone conformation.

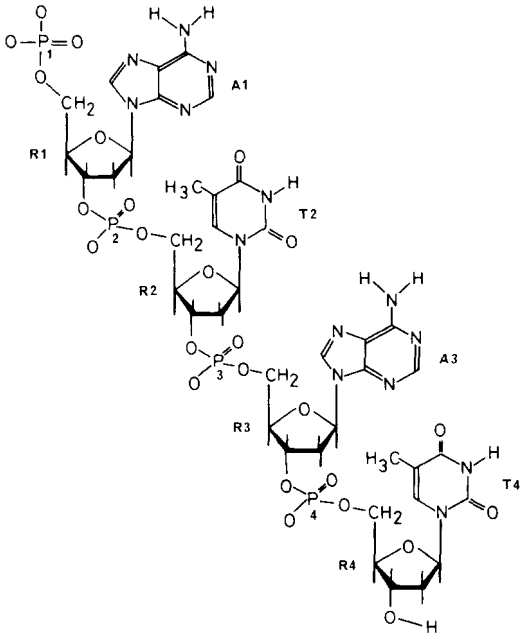

Fig. 1. Chemical formula and residue numbering.

EXPERIMENTAL

d-pApTpApT was synthesized by chemically polymerizing the dinucleotide d-pApT using the diester approach.[8] The material was purified by ion-exchange chromatography on columns of DEAE cellulose. The ammonium salt of the deoxytetranucleotide was crystallized at pH 7.5 as fine needles on diffusion of acetone into the aqueous solution over a period of about 2 weeks. The crystals were extremely hygroscopic and also readily damaged in the presence of excess acetone. After many attempts an undamaged single crystal was sealed in a capillary tube with mother liquor containing some additional acetone, and this was used for all experimental work.

The crystals were monoclinic with space group $P2_1$ and cell constants $a = 21.121\ (10), b = 21.294\ (14), c = 8.770\ (4)$ Å, $\beta = 97.84\ (4)°$. The density, measured in a bromoform–xylene gradient column was 1.525 (5) g cm^{-3}, indicating the presence of two oligomers and 62 species with M_r = 18 (H_2O or NH_4^+) in the unit cell (d_{cal} = 1.52 g cm^{-3}). Intensities were measured on a Syntex $P2_1$ diffractometer by the $\omega/2\theta$ scan technique using a high-intensity x-ray tube with monochromatized MoK_α radiation. The resolution was 1.04 Å ($2\theta_{max} = 40°$). There were no significant changes in the intensities of two monitor reflections during data collection. Measurements were made at 4528 reciprocal lattice points, giving 2717 independent reflections with $F \geq 1.5\sigma(F)$. These were used, after the usual corrections, for the solution and refinement of the structure.

d-pApTpApT has a self-complementary base sequence. Theoretically, therefore, it could crystallize as a self-paired duplex of four base pairs. The present structure, however, contained two oligomers related by a two-fold screw axis, which ruled out this possibility and suggested that the actual structure would be significantly different from the usual double helix.

Determination of the structure was not straightforward. Initially we attempted to solve the phase problem by direct methods using both the SHELX and the MULTAN[9] sets of programs in combination with a wide variety of modifications to the starting phase set. Some of the E-maps obtained from these calculations contained covalently linked planar fragments corresponding to adenine. All attempts to derive the structure from phase expansions based on these fragments failed.

As an alternative, skeletal and CPK models of the tetranucleotide were built and positioned in the unit cell with the bases oriented along the (604) plane (which had the highest E_{obs} value). Information on the packing of RNA double-helical fragments ApU[10] and GpC,[11,12] which crystallize in the same space group, was also used. The model and its orientation were adjusted with due regard to the restrictions imposed by the short 8.8-Å c axis to enable the generation of Watson-Crick-type base pairs by suitable screw rotations and cell translations. From these considerations, a tetranucleotide model consisting of two helical dinucleotide units seemed most favorable. However, the nature of the link between the two units was not clear at that stage. This model served as a guide in locating the posi-

tions of the P atoms from a sharpened Patterson map. Phases generated for the two P atoms that could be located most precisely were used as a starting point for tangent expansion following closely the method described by Karle.[13] An almost complete structure was generated in six cycles. The remaining atoms, as well as the water molecules (some possibly NH_4^+ ions), distributed among 42 sites, were located from difference maps.

The structure was refined by least-squares to a conventional $R = 0.153$. The site occupancies of the water molecule/NH_4^+ ions were included among the variables. It was decided to refine the site occupanies of the solvent molecules rather than their temperature factors, since several water–water contacts were shorter than 2 Å, indicating that the water molecules are disordered. Thirty-six H atoms of the tetranucleotide molecule were fixed at calculated positions. Only P atoms were allowed anisotropic temperature factors. It was not possible to refine the structure further because of the disordered water, and the limited data set.

A view of the molecule perpendicular to the bases is given in Fig. 2. It shows that the molecule is extended about the middle phosphodiester link.

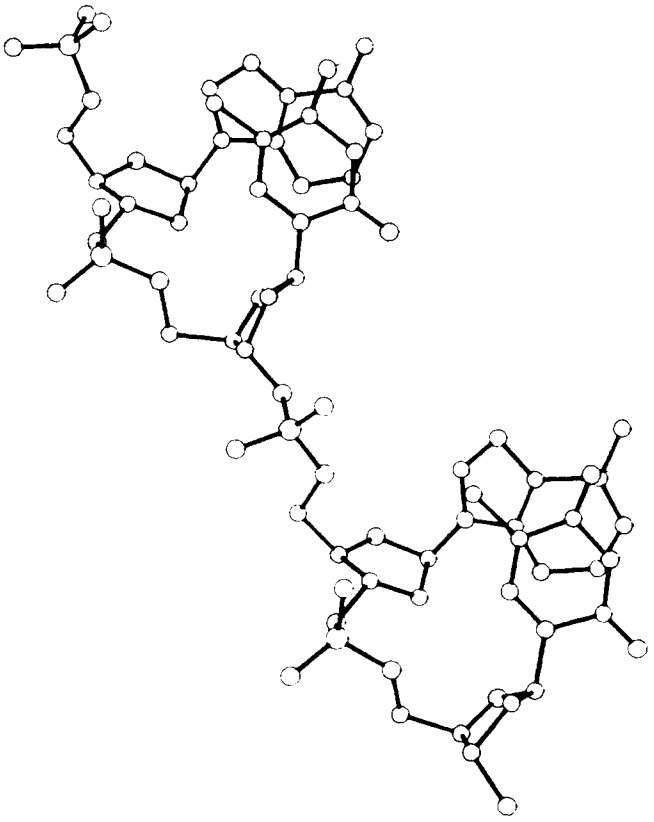

Fig. 2. PLUTO drawing of a single molecule viewed perpendicular to the bases.

The two halves on either side have very similar conformations. All four nucleotide units have the normal *gg* conformation about the C4′–C5′ bond.

The final coordinates and thermal parameters of non-hydrogen atoms are listed in Tables I and II; bond lengths and angles are given in Table III.

RESULTS AND DISCUSSION

Double-Helical Fragment

The oligomer molecule, as mentioned under Experimental, cannot form a self-complementary double helix of four base pairs in the present structure, which only has a 2_1 symmetry operator. A segment of a right-handed, antiparallel, two-base-pair double helix is, however, formed with complementary hydrogen bonding between adenine and thymine bases from two molecules related by the 2_1 axis (A1·T4*, T2·A3*; starred bases at $1 - x$, $-\frac{1}{2} + y$, $-z$). The converse pairs T4·A1* and A3·T2* have the starred bases at $1 - x$, $\frac{1}{2} + y$, $-z$; thus each molecule contributes to two minihelices, one with each of two other molecules related by a y translation.

Figure 3 gives views of this minihelix perpendicular and parallel to the base pairs. Each base pair is held by hydrogen bonds between the N6 amino group of adenine and the O4 carbonyl group of thymine (3.04 Å av.) and between N1 of adenine and N3 of thymine (2.82 Å av.) in the classical Watson-Crick geometry, which is seen here for the first time for adenine–thymine at atomic resolution in a single-crystal study.

Within each base pair the pyrimidine and purine bases are inclined to each other with a dihedral angle of 13° between A1 and T4* and 14° between T2 and A3*. A similar propeller twist that increases the overlap between one base and its neighbors is observed in the dodecamer d(CGCGAATTCGCG)[7] and was proposed by Levitt from energy calculations.[14] The mean planes through the base pairs A1·T4* and T2·A3* are nearly parallel to each other (3°), with a vertical separation of 3.34 Å. The angular orientation of the base pairs, defined by the angle between vectors C1′R1-C1′R4* and C1′R2-C1′R3*, is 31°, and the C1′-C1′ interstrand separation is 10.2 Å, close to that found in ApU.[10] This distance is significantly shorter than the corresponding distance found in the structure of GpC.[11,12]

Sugar Conformation and Sugar–Base Orientation

A striking feature of the d-pApTpApT molecule, and hence of the minihelix, is the alternation of the sugar conformation between C3′-*endo* and C2′-*endo* pucker, depending on whether the sugar is attached to a purine or pyrimidine base. This is in contrast to the classical interpretations of DNA fiber patterns based on monotonic sugar geometry, C3′-*endo* in A-DNA and C2′-*endo* in B-DNA.[2]

TABLE I
Atomic Coordinates and Isotropic Temperature Factors[a]

Atom	$10^4x/a$	$10^4y/b$	$10^4z/c$	10^3U
P4	1399(4)	7400(6)	−815(13)	*
O1P4	1304(11)	6786(12)	−1700(26)	101(8)
O2P4	863(13)	7758(13)	−376(30)	127(9)
O3P4	1868(9)	7331(9)	681(21)	67(6)
O5P4	1777(9)	7825(10)	−1790(22)	81(6)
P3	1803(4)	5031(4)	1511(10)	*
O1P3	1892(11)	4771(12)	171(29)	111(8)
O2P3	1140(9)	5165(9)	1799(21)	69(6)
O3P3	2158(7)	4658(8)	2871(17)	47(5)
O5P3	2211(8)	5626(8)	1569(18)	56(5)
P2	1045(4)	2843(5)	6669(9)	*
O1P2	496(12)	3221(12)	7106(27)	112(8)
O2P2	887(8)	2262(10)	5805(20)	65(5)
O3P2	1448(9)	2712(9)	8264(21)	70(6)
O5P2	1499(7)	3220(8)	5698(18)	48(5)
P1	1535(5)	322(0)	8781(12)	*
O1P1	1588(13)	87(14)	7263(34)	136(10)
O2P1	918(18)	242(19)	9266(42)	191(14)
O3P1	2106(24)	−61(26)	9932(60)	298(23)
O5P1	1759(8)	1017(8)	8839(19)	57(5)
O1R4	3001(10)	8382(11)	−2324(23)	85(6)
C1R4	2997(14)	8265(15)	−3942(33)	71(9)
C2R4	2393(11)	8275(12)	−4791(29)	47(7)
C3R4	2066(17)	8796(18)	−3905(38)	100(11)
O3R4	2229(12)	9451(13)	−4583(30)	122(9)
C4R4	2451(13)	8721(14)	−2300(30)	65(9)
C5R4	1973(16)	8420(16)	−1280(37)	85(10)
O1R3	3179(8)	6565(9)	2746(19)	58(5)
C1R3	3578(11)	6889(12)	1791(27)	43(7)
C2R3	3064(13)	7258(16)	776(35)	80(9)
C3R3	2427(9)	6943(10)	798(23)	26(6)
C4R3	2554(12)	6672(13)	2481(29)	55(7)
C5R3	2156(13)	6100(14)	2852(31)	60(8)
O1R2	2697(8)	3590(8)	5191(18)	53(5)
C1R2	2738(12)	3364(13)	3574(29)	49(8)
C2R2	2141(16)	3503(18)	2819(41)	97(11)
C3R2	1917(12)	4112(12)	3519(28)	50(7)
C4R2	2210(11)	4044(12)	5003(27)	43(7)
C5R2	1716(16)	3875(17)	6231(39)	97(11)
O1R1	2708(9)	1846(10)	10383(22)	82(6)
C1R1	3129(12)	2202(13)	9405(27)	47(7)
C2R1	2638(12)	2631(14)	8441(32)	62(8)
C3R1	1984(11)	2316(12)	8473(28)	45(7)
C4R1	2015(10)	2029(11)	9935(25)	36(6)
C5R1	1684(12)	1431(12)	10058(28)	52(8)
N1T4	3289(11)	7601(11)	−3820(26)	66(7)
C2T4	3908(12)	7505(13)	−4450(29)	50(7)
O2T4	4179(8)	7969(9)	−4892(20)	67(5)

(*continued*)

TABLE I (*continued*)

Atom	$10^4x/a$	$10^4y/b$	$10^4z/c$	10^3U
N3T4	4078(10)	6902(11)	−4475(23)	54(6)
C4T4	3774(12)	6383(13)	−4026(27)	43(7)
O4T4	4059(9)	5907(10)	−4154(23)	80(6)
C5T4	3189(12)	6518(13)	−3441(27)	45(7)
C6T4	2965(10)	7100(11)	−3478(24)	33(6)
C7T4	2828(13)	5945(14)	−2849(32)	69(8)
N1A3	5307(8)	6744(9)	−1620(20)	36(5)
C2A3	5002(10)	7222(13)	−1165(25)	41(6)
N3A3	4508(10)	7191(11)	−209(25)	68(7)
C4A3	4320(13)	6623(14)	132(31)	58(8)
C5A3	4526(14)	6057(16)	−357(33)	67(9)
C6A3	5153(14)	6144(15)	−1210(32)	68(9)
N6A3	5401(12)	5583(13)	−1742(28)	87(8)
N7A3	4256(9)	5528(10)	218(22)	46(6)
C8A3	3910(12)	5847(13)	954(29)	51(7)
N9A3	3876(11)	6444(12)	889(25)	65(7)
N1T2	2949(9)	2735(10)	3726(22)	47(6)
C2T2	3532(13)	2571(14)	3297(31)	56(8)
O2T2	3875(9)	2971(10)	2806(21)	71(6)
N3T2	3672(10)	1950(11)	3280(23)	51(6)
C4T2	3224(14)	1477(16)	3707(33)	67(9)
O4T2	3473(9)	950(9)	3425(20)	66(5)
C5T2	2706(13)	1686(14)	4227(31)	62(8)
C6T2	2567(10)	2276(11)	4219(22)	26(6)
C7T2	2255(12)	1201(13)	4707(30)	60(8)
N1A1	4831(9)	1805(11)	6019(23)	54(6)
C2A1	4619(13)	2337(15)	6598(30)	67(8)
N3A1	4100(10)	2377(12)	7380(25)	70(7)
C4A1	3929(10)	1799(11)	7706(24)	31(6)
C5A1	4072(11)	1246(12)	7384(26)	44(7)
C6A1	4582(11)	1243(12)	6338(27)	38(7)
N6A1	4811(13)	753(15)	5870(31)	95(9)
N7A1	3735(10)	801(11)	7794(24)	60(7)
C8A1	3344(11)	1053(12)	8595(27)	40(7)
N9A1	3423(10)	1699(11)	8622(23)	61(6)

* Anisotropic Temperature Factors ($\times 10^3$)[a]

	U_{11}	U_{22}	U_{33}	U_{23}	U_{13}	U_{12}
P4	65(6)	121(10)	129(8)	56(8)	58(6)	37(6)
P3	92(7)	55(6)	58(5)	−1(5)	−1(5)	6(5)
P2	49(5)	90(7)	59(5)	9(5)	24(4)	−13(5)
P1	111(8)	76(7)	96(8)	−14(6)	28(6)	3(6)

[a] Temperature factor units are Å^2. The temperature factor exponent takes the following form: $-2\pi^2(U_{11}h^2a^{*2} + \cdots + 2U_{12}hka^*b^*)$.

The relative orientations of the base and sugar, defined by the glycosidic torsion angles χ_{CN}, are *anti* for the four bases. The χ_{CN} values are almost at the limits of those found in single-crystal studies[15]: O1′-Cl′-N9-C8, 5° (A1) and −9° (A3) and O1′-C1′-N1-C6, 69° (T2) and 75° (T4). A negative

TABLE II
Water/Ammonium Ion Coordinates and Site Occupation Factors (α)[a]

	$10^4x/a$	$10^4y/b$	$10^4z/c$	α
Ow1	9082(15)	7143(17)	7297(36)	0.97(4)
Ow2	1230(14)	6902(16)	5039(35)	1.05(4)
Ow3	214(22)	9163(24)	5603(53)	0.65(4)
Ow4	9383(25)	5915(27)	4487(61)	0.58(4)
Ow5	6442(39)	9855(42)	6402(96)	0.37(4)
Ow6	1297(18)	5465(20)	7593(44)	0.77(4)
Ow7	4138(26)	8452(28)	512(64)	0.56(4)
Ow8	643(32)	5150(45)	4799(80)	0.47(5)
Ow9	6949(19)	9217(21)	42(47)	0.76(4)
Ow10	648(38)	5646(53)	4561(91)	0.43(5)
Ow11	6316(24)	9671(26)	4815(59)	0.62(4)
Ow12	5855(42)	4442(47)	2902(102)	0.38(4)
Ow13	824(29)	7890(34)	2827(73)	0.49(4)
Ow14	804(35)	5582(39)	8282(82)	0.41(4)
Ow15	6123(24)	8825(27)	2007(61)	0.69(4)
Ow16	5913(36)	8412(42)	1109(93)	0.42(4)
Ow17	1283(24)	9355(26)	2340(58)	0.61(4)
Ow18	774(43)	7124(49)	2944(104)	0.35(4)
Ow19	58(28)	6405(29)	8145(64)	0.54(4)
Ow20	3572(31)	8728(33)	2383(75)	0.49(4)
Ow21	9419(23)	9089(25)	723(54)	0.64(4)
Ow22	9758(23)	8257(27)	8620(58)	0.61(4)
Ow23	2763(35)	9819(38)	2362(85)	0.44(4)
Ow24	4244(33)	4272(34)	1925(77)	0.49(4)
Ow25	9492(40)	5779(43)	7801(95)	0.37(4)
Ow26	5315(62)	4275(60)	4238(132)	0.29(4)
Ow27	4896(49)	3634(56)	3460(118)	0.31(4)
Ow28	4636(58)	4204(56)	4397(126)	0.30(4)
Ow29	4712(40)	4296(41)	909(92)	0.39(4)
Ow30	210(40)	4525(47)	6458(95)	0.37(4)
Ow31	3622(48)	9544(51)	7293(134)	0.34(5)
Ow32	4762(47)	8879(55)	3363(117)	0.32(5)
Ow33	50(69)	5499(72)	9290(154)	0.23(4)
Ow34	5370(48)	4533(56)	557(123)	0.30(4)
Ow35	3516(26)	9696(29)	4953(64)	0.57(4)
Ow36	6893(42)	9455(47)	1056(103)	0.36(4)
Ow37	9828(54)	7130(61)	658(133)	0.28(4)
Ow38	5005(45)	9244(51)	2473(111)	0.37(4)
Ow39	246(32)	6127(38)	853(83)	0.46(4)
Ow40	262(52)	6579(59)	2832(134)	0.28(4)
Ow41	9203(45)	4969(49)	4989(113)	0.33(4)
Ow42	9966(45)	6314(50)	3859(107)	0.37(14)

[a] All isotropic temperature factors fixed at 0.15 Å^2.

value for χ is particularly uncommon and has been observed in 5′-dCMP ($-6°$),[16] where, however, the sugar is C3′-*exo*. It should be noted that the sugar conformation in the left-handed d(CG)$_3$ structure[4] also alternates between C2′-*endo* and C3′-*endo* for pyrimidines and purines, respectively, whereas the corresponding glycosidic angles exhibit the *anti* and *syn*

TABLE III
Bond Lengths (Å) and Bond Angles (deg)

Atoms	Bond Length	Atoms	Bond Length
P4-O1P4	1.52(3)	P4-O2P4	1.46(3)
P4-O3P4	1.54(2)	P4-O5P4	1.54(2)
P3-O1P3	1.34(3)	P3-O2P3	1.48(2)
P3-O3P3	1.54(2)	P3-O5P3	1.53(2)
P2-O1P2	1.50(3)	P2-O2P2	1.47(2)
P2-O3P2	1.56(2)	P2-O5P2	1.58(2)
P1-O1P1	1.44(3)	P1-O2P1	1.44(4)
P1-O3P1	1.67(5)	P1-O5P1	1.55(2)
C1R4-O1R4	1.44(4)	C1R4-C2R4	1.39(4)
C1R4-N1T4	1.54(4)	C2R4-C3R4	1.57(5)
C3R4-O3R4	1.57(5)	C3R4-C4R4	1.54(4)
C4R4-O1R4	1.37(4)	C4R4-C5R4	1.57(5)
C5R4-O5P4	1.39(4)	C1R3-O1R3	1.44(3)
C1R3-C2R3	1.53(4)	C1R3-N9A3	1.43(4)
C2R3-C3R3	1.51(4)	C3R3-O3P4	1.43(3)
C3R3-C4R3	1.57(3)	C4R3-O1R3	1.33(3)
C4R3-C5R3	1.54(4)	C5R3-O5P3	1.53(3)
C1R2-O1R2	1.51(3)	C1R2-C2R2	1.37(4)
C1R2-N1T2	1.41(3)	C2R2-C3R2	1.54(5)
C3R2-O3P3	1.42(3)	C3R2-C4R2	1.37(3)
C4R2-O1R2	1.41(3)	C4R2-C5R2	1.64(5)
C5R2-O5P2	1.52(4)	C1R1-O1R1	1.52(3)
C1R1-C2R1	1.55(4)	C1R1-N9A1	1.46(4)
C2R1-C3R1	1.54(4)	C3R1-O3P2	1.40(3)
C3R1-C4R1	1.41(3)	C4R1-O1R1	1.51(3)
C4R1-C5R1	1.46(4)	C5R1-O5P1	1.41(3)
C2T4-N1T4	1.50(4)	C2T4-O2T4	1.23(3)
C2T4-N3T4	1.34(4)	C4T4-N3T4	1.36(4)
C4T4-O4T4	1.19(3)	C4T4-C5T4	1.43(4)
C5T4-C6T4	1.33(4)	C5T4-C7T4	1.56(4)
C6T4-N1T4	1.56(4)	C2A3-N1A3	1.30(3)
C2A3-N3A3	1.43(3)	C4A3-N3A3	1.32(4)
C4A3-C5A3	1.37(4)	C4A3-N9A3	1.28(4)
C5A3-C6A3	1.62(4)	C5A3-N7A3	1.39(4)
C6A3-N7A3	1.38(4)	C6A3-N6A3	1.41(4)
C8A3-N7A3	1.24(4)	C8A3-N9A3	1.27(4)
C2T2-N1T2	1.38(4)	C2T2-O2T2	1.23(4)
C2T2-N3T2	1.36(4)	C4T2-N3T2	1.47(4)
C4T2-O4T2	1.28(4)	C4T2-C5T2	1.32(4)
C5T2-C6T2	1.29(4)	C5T2-C7T2	1.50(4)
C6T2-N1T2	1.37(3)	C2A1-N1A1	1.34(4)
C2A1-N3A1	1.37(4)	C4A1-N3A1	1.32(4)
C4A1-C5A1	1.26(4)	C4A1-N9A1	1.44(3)
C5A1-C6A1	1.51(4)	C5A1-N7A1	1.27(3)
C6A1-N1A1	1.35(3)	C6A1-N6A1	1.24(4)
C8A1-N7A1	1.27(3)	C8A1-N9A1	1.38(3)

(*continued*)

TABLE III (*continued*)

Atoms	Bond Angle	Atoms	Bond Angle
O1P4-P4-02P4	122(2)	O1P4-P4-O3P4	112(1)
O1P4-P4-05P4	105(1)	O2P4-P4-O3P4	105(1)
O2P4-P4-05P4	109(2)	O3P4-P4-O5P4	102(1)
O1P3-P3-O2P3	119(1)	O1P3-P3-O3P3	111(1)
O1P3-P3-O5P3	103(1)	O2P3-P3-O3P3	110(1)
O2P3-P3-O5P3	112(1)	O5P3-P3-O3P3	101(1)
O1P2-P2-O2P2	117(1)	O1P2-P2-O3P2	102(1)
O1P2-P2-O5P2	114(1)	O2P2-P2-O3P2	112(1)
O2P2-P2-O5P2	105(1)	O3P2-P2-O5P2	106(1)
O1P1-P1-O2P1	115(2)	O1P1-P1-O3P1	104(2)
O1P1-P1-O5P1	107(2)	O2P1-P1-O3P1	112(3)
O2P1-P1-O5P1	113(2)	O3P1-P1-O5P1	105(2)
P4-O3P4-C3R3	123(2)	P4-O5P4-C5R4	121(2)
P3-O3P3-C3R2	125(1)	P3-O5P3-C5R3	118(2)
P2-O3P2-C3R1	124(2)	P2-O5P2-C5R2	119(2)
P1-O5P1-C5R1	124(2)	C1R4-O1R4-C4R4	102(2)
O1R4-C1R4-C2R4	114(3)	O1R4-C1R4-N1T4	98(2)
C2R4-C1R4-N1T4	112(2)	C1R4-C2R4-C3R4	100(2)
C2R4-C3R4-O3R4	108(3)	C2R4-C3R4-C4R4	100(3)
O3R4-C3R4-C4R4	109(3)	O1R4-C4R4-C3R4	113(3)
O1R4-C4R4-C5R4	114(2)	C3R4-C4R4-C5R4	105(2)
O5P4-C5R4-C4R4	112(3)	C1R3-O1R3-C4R3	118(2)
O1R3-C1R3-C2R3	99(2)	O1R3-C1R3-N9A3	110(2)
C2R3-C1R3-N9A3	110(2)	C1R3-C2R3-C3R3	109(2)
O3P4-C3R3-C2R3	118(2)	O3P4-C3R3-C4R3	108(2)
C2R3-C3R3-C4R3	98(2)	O1R3-C4R3-C3R3	105(2)
O1R3-C4R3-C5R3	113(2)	C3R3-C4R3-C5R3	117(2)
O5P3-C5R3-C4R3	106(2)	C1R2-O1R2-C4R2	104(2)
O1R2-C1R2-C2R2	103(2)	O1R2-C1R2-N1T2	106(2)
C2R2-C1R2-N1T2	121(3)	C1R2-C2R2-C3R2	108(3)
O3P3-C3R2-C2R2	113(2)	O3P3-C3R2-C4R2	109(2)
C2R2-C3R2-C4R2	100(2)	O1R2-C4R2-C3R2	114(2)
O1R2-C4R2-C5R2	107(2)	C3R2-C4R2-C5R2	114(2)
O5P2-C5R2-C4R2	101(2)	C1R1-O1R1-C4R1	110(2)
O1R1-C1R1-C2R1	102(2)	O1R1-C1R1-N9A1	103(2)
C2R1-C1R1-N9A1	118(2)	C1R1-C2R1-C3R1	106(2)
O3P2-C3R1-C2R1	116(2)	O3P2-C3R1-C4R1	108(2)
C2R1-C3R1-C4R1	106(2)	O1R1-C4R1-C3R1	106(2)
O1R1-C4R1-C5R1	102(2)	C3R1-C4R1-C5R1	119(2)
O5P1-C5R1-C4R1	113(2)	C1R4-N1T4-C2T4	117(2)
C1R4-N1T4-C6T4	123(2)	C2T4-N1T4-C6T4	118(2)
N1T4-C2T4-O2T4	118(2)	N1T4-C2T4-N3T4	113(2)
O2T4-C2T4-N3T4	129(3)	C2T4-N3T4-C4T4	130(2)
N3T4-C4T4-O4T4	114(2)	N3T4-C4T4-C5T4	114(2)
O4T4-C4T4-C5T4	133(3)	C4T4-C5T4-C6T4	120(2)
C4T4-C5T4-C7T4	117(2)	C6T4-C5T4-C7T4	123(2)
N1T4-C6T4-C5T4	124(2)	C2A3-N1A3-C6A3	120(2)
N1A3-C2A3-N3A3	125(2)	C2A3-N3A3-C4A3	116(2)
N3A3-C4A3-C5A3	128(3)	N3A3-C4A3-N9A3	131(3)
C5A3-C4A3-N9A3	101(3)	C4A3-C5A3-C6A3	111(3)

(*continued*)

TABLE III (*continued*)

Atoms	Bond Angle	Atoms	Bond Angle
C4A3-C5A3-N7A3	116(3)	C6A3-C5A3-N7A3	132(3)
N1A3-C6A3-C5A3	118(3)	N1A3-C6A3-N6A3	126(3)
C5A3-C6A3-N6A3	115(3)	C5A3-N7A3-C8A3	93(2)
N7A3-C8A3-N9A3	124(3)	C1R3-N9A3-C4A3	120(3)
C1R3-N9A3-C8A3	131(2)	C4A3-N9A3-C8A3	106(3)
C1R2-N1T2-C2T2	120(2)	C1R2-N1T2-C6T2	121(2)
C2T2-N1T2-C6T2	119(2)	N1T2-C2T2-O2T2	121(3)
N1T2-C2T2-N3T2	117(2)	O2T2-C2T2-N3T2	122(3)
C2T2-N3T2-C4T2	121(2)	N3T2-C4T2-O4T2	105(2)
N3T2-C4T2-C5T2	117(3)	O4T2-C4T2-C5T2	138(3)
C4T2-C5T2-C6T2	122(3)	C4T2-C5T2-C7T2	117(3)
C6T2-C5T2-C7T2	121(3)	N1T2-C6T2-C5T2	124(2)
C2A1-N1A1-C6A1	121(2)	N1A1-C2A1-N3A1	125(3)
C2A1-N3A1-C4A1	108(2)	N3A1-C4A1-C5A1	138(3)
N3A1-C4A1-N9A1	120(2)	C5A1-C4A1-N9A1	102(2)
C4A1-C5A1-C6A1	111(2)	C4A1-C5A1-N7A1	118(2)
C6A1-C5A1-N7A1	130(2)	N1A1-C6A1-C5A1	117(2)
N1A1-C6A1-N6A1	120(3)	C5A1-N6A1-N6A1	123(3)
C5A1-N7A1-C8A1	106(2)	N7A1-C8A1-N9A1	110(2)
C1R1-N9A1-C4A1	124(2)	C1R1-N9A1-C8A1	133(2)
C4A1-N9A1-C8A1	104(2)		

conformations. However, with the same glycosidic orientations, the sugar conformation in the $d(CG)_2$ structure[5,6] alternates between C2′-*endo* and C1′-*exo* for deoxycytidine and deoxyguanosine, respectively.

All these findings suggest that it may be necessary to take into account irregular or periodic variations in sugar–base orientation and sugar pucker parameters, at least over local regions of double-helical structures, depending on the nature of the nucleotide sequence.

The Sugar–Phosphate Backbone

Figure 4 shows schematically the conformation of the sugar–phosphate backbone. The value of the torsional angle ψ about the C3′-C4′ bond depends on the sugar conformation and thus alternates along the backbone. The torsion angles ω and ω' about the P-O5′ and P-O3′ ester bonds in the d(A-T) fragments are close to those allowed for right-handed double-helical polynucleotides. The conformation of the backbone within the two halves of the molecule is remarkably similar. The phosphodiester linkage between R2 and R3, however, is very different, with a *trans–gauche* (tg^-) conformation about the P3-O3′ and P3-O5′ bonds. This conformation gives rise to an extended backbone, similar to that observed in the crystal structures UpA[17,18] and pTpT.[19] In the present structure, however, the ψ values of R2 and R3 are different, since they relate to the sugar conformation.

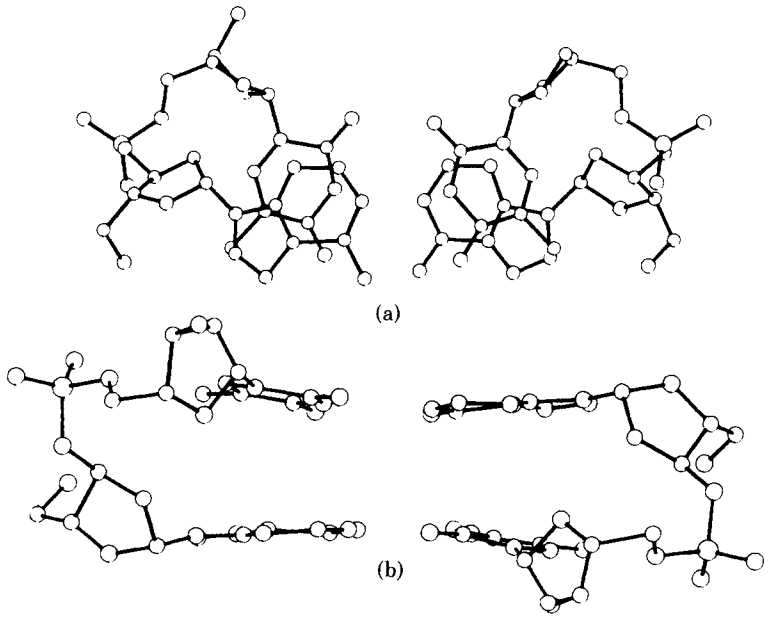

Fig. 3. (a) The minihelix formed by two molecules related by a 2_1 axis, viewed perpendicular to the bases. (b) The minihelix viewed parallel to the bases.

The dimensions of the phosphate group are similar to those observed in the crystal structures of nucleotides containing the phosphodiester linkage. The free P-O bonds are short and the valence angles large (1.45 Å av., O1-P-O2 = 118° av.) compared with the ester bonds and angles (1.54 Å av., O3-P-O5 = 104° av.). The valence angles at O3′ and O5′ are close to 120°. It should, however, be noted that the high thermal parameters of some phosphate oxygens may make some phosphate dimensions imprecise.

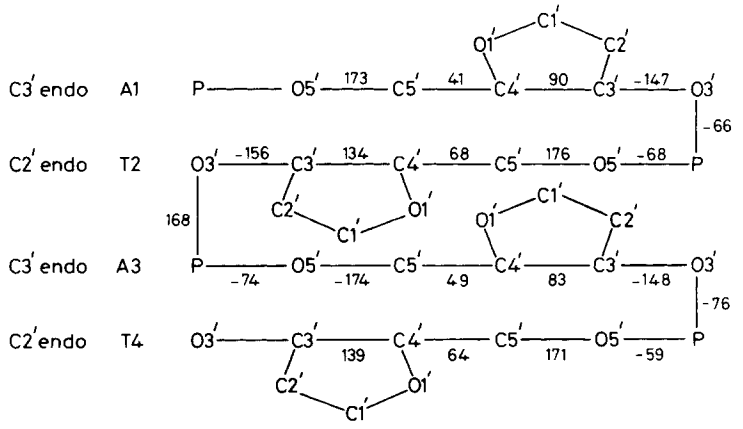

Fig. 4. Schematic view of the sugar–phosphate backbone.

Base Stacking and Extended Crystal Structure

Base stacking contributes an important stabilizing force in polynucleotide structure. In d-pApTpApT the conformation of each molecule is stabilized by the considerable overlap between the adenine and thymine bases in the two halves of the molecule and also between the adenines A3 and A1* of two molecules related by a 2_1 axis. The average vertical distance between these bases is 3.5 Å. The extended structure is further stabilized by intermolecular base–sugar interactions, similar to those found in UpA.[17,18] Intramolecular base–sugar stacking was observed in $d(CG)_3$[4] and $d(CG)_2$ structures.[4–6] The stacking arrangements formed in the present structure are shown in the stereo views, Fig. 5(a,b). To place the degree of overlap on a semiquantitative basis, we used potential-energy calculations,[20] which sum the interaction energy between selected atomic groupings. We find that all three interactions A1:T2, A3:T4, and A3:A1* are −5.2 kcal/mol.

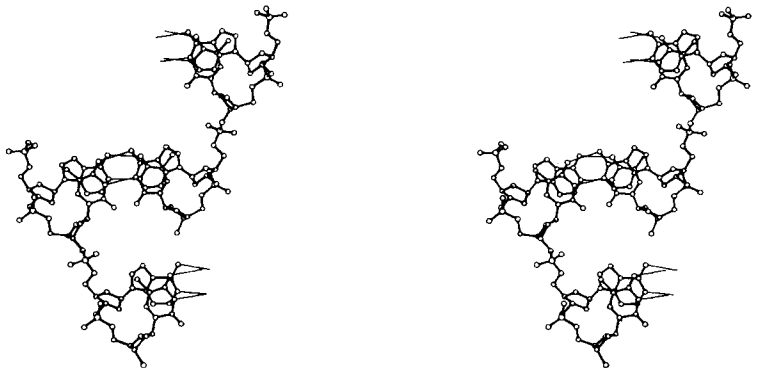

(a)

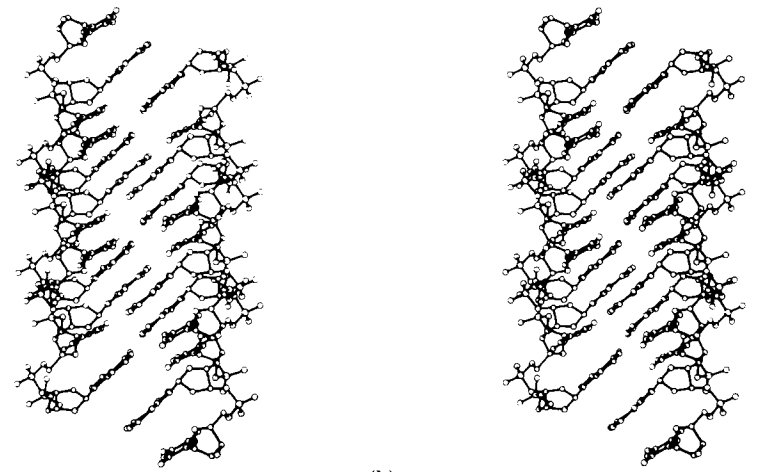

(b)

Fig. 5. (a) Stereodiagram of the two molecules related by the 2_1 screw axis. (b) Stereodiagram of the extended crystal structure showing base–base and base–sugar interactions.

The interaction energy between thymine and ribose, related by a c translation, is −3.9 kcal/mol between T2 and R1* and −3.4 kcal/mol between T4 and R3* (starred sugars at $x, y, -1 + z$). These figures are only approximate, but they do indicate the relative contributions of the various interactions.

In addition to these stacking forces, the molecules related by the b translation are held head to tail by a hydrogen bond 2.62 Å long between the O3′ hydroxyl group of one molecule at x, y, z and the free 5′-terminal phosphate oxygen atom O1P1 of a molecule at $x, 1 + y, 1 + z$.

The extended crystal structure is stabilized by the water molecules and the NH_4^+ ions. Hydrogen-bond distances of the first hydration shell are given in Table IV. All the free phosphate oxygens are coordinated by water/NH_4^+ ions, and so are the two oxygen atoms of the thymine and N3, N6, and N7 of the adenine bases. In addition, the O1′ atoms of the deoxyribose rings of the thymines are coordinated to water molecules Ow11 (3.1 Å) and Ow31 (2.8 Å). There is also a network of hydrogen bonds between the water molecules forming a partially ordered structure that extends in infinite columns along the c axis parallel to the water-free columns of stacked base pairs as illustrated in Fig. 6. This structured water provides a major stabilizing force maintaining the d-pApTpApT molecule in the extended crystal structure and accounts for the extreme instability of the crystals in the absence of the mother liquor of precise water content.

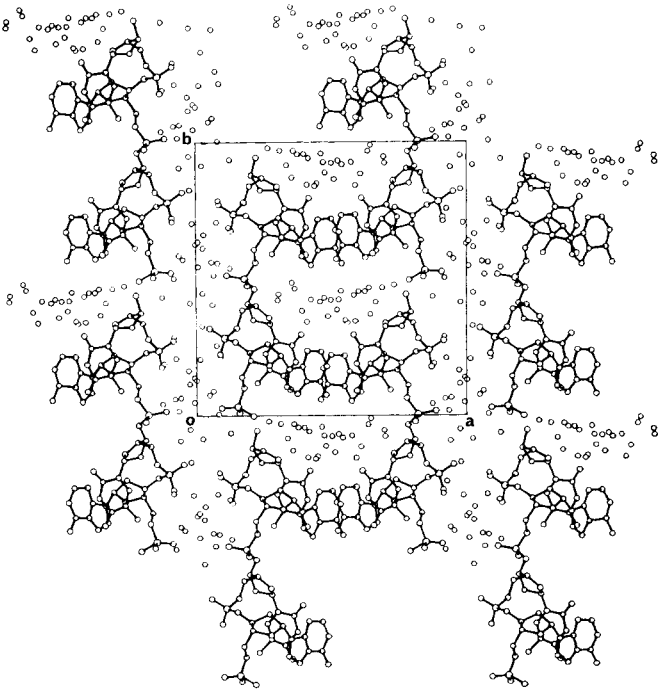

Fig. 6. Packing diagram of the extended crystal structure projected down the c axis. Water oxygens and N atoms of the NH_4^+ groups are shown as unconnected circles.

TABLE IV
Hydrogen-Bond Contacts of the First Hydration Shell[a]

	Distance (Å)	Symmetry Element	Translation Along		
			a	*b*	*c*
O1P4···Ow2	2.85	1	0	0	−1
O1P4···Ow6	2.88	1	0	0	−1
O1P4···Ow14	2.77	1	0	0	−1
O1P4···Ow19	2.74	1	0	0	−1
O2P4···Ow13	2.84	1	−1	0	0
O2P4···Ow22	2.61	1	−1	0	−1
O2P4···Ow37	2.82	1	−1	0	0
O1P3···Ow6	2.85	1	0	0	−1
O1P3···Ow9	2.75	2	1	−1	0
O1P3···Ow21	3.13	2	1	−1	0
O1P3···Ow36	2.99	2	1	−1	0
O2P3···Ow8	2.96	1	0	0	0
O2P3···Ow10	2.95	1	0	0	0
O2P3···Ow33	3.04	1	−1	0	−1
O2P3···Ow39	2.83	1	−1	0	0
O3P3···Ow5	2.97	2	1	−1	1
O1P2···Ow13	2.88	2	1	−1	1
O1P2···Ow21	2.64	2	1	−1	1
O1P2···Ow30	2.88	1	0	0	0
O2P2···Ow1	2.74	2	1	−1	1
O2P2···Ow4	2.93	2	1	−1	1
O2P2···Ow42	2.75	2	1	−1	1
O1P1···Ow4	2.97	2	1	−1	1
O1P1···Ow41	2.42	2	1	−1	1
O2P1···Ow25	3.05	2	1	−1	2
O2P1···Ow33	2.61	2	1	−1	2
O2P1···Ow39	3.09	2	1	−1	1
O3P1···Ow23	2.39	1	0	−1	1
O1R4···Ow31	2.84	2	1	0	0
O3R4···Ow17	3.14	1	0	0	−1
O3R4···Ow35	2.85	1	0	0	−1
O1R2···Ow11	3.11	2	1	−1	1
O2T4···Ow20	3.02	1	0	0	−1
O2T4···Ow26	3.01	2	1	0	0
O2T4···Ow27	2.60	2	1	0	0
O2T4···Ow32	2.85	1	0	0	−1
O4T4···Ow5	3.08	2	1	−1	0
O4T4···Ow11	2.79	2	1	−1	0
N3A3···Ow7	2.89	1	0	0	0
N6A3···Ow34	2.98	1	0	0	0
N6A3···Ow38	3.02	2	1	−1	0
N7A3···Ow24	3.07	1	0	0	0
N7A3···Ow29	2.83	1	0	0	0
N7A3···Ow34	3.12	1	0	0	0
O2T2···Ow24	3.01	1	0	0	0
O2T2···Ow27	2.58	1	0	0	0
O4T2···Ow23	2.92	1	0	−1	0
O4T2···Ow35	2.98	1	0	−1	0
N3A1···Ow16	2.57	2	1	−1	1
N7A1···Ow12	3.11	2	1	−1	1
N7A1···Ow31	2.72	2	1	−1	1

[a] The second atom in each pair is related to the first by the corresponding symmetry and translation: (1) x, y, z; (2) $-x$, (1/2) $+y, -z$. The average esd is 0.08 Å.

Poly(dA-dT) Model

The minihelix (A1-T2)·(A3*-T4*) found in the crystal structure provides a starting point for generating various models for the (dA-dT) copolymer. The coordinates of the minihelix are given in Table V. We have generated a right-handed double helix with the helix axis passing through the base pairs. Models built by hand and using computer programs[21] showed that no helical structure could be generated from the crystal structure by helical rotation and translation only; it was necessary to make a major change in the conformation of the phosphodiester bridge between T2 and A3 (ω', the torsion angle about the O3′-P bond, being changed from 168° to −125°; and ϕ, the torsion angle about the C3′-O3′ bond, from −156° to −175°). The resultant polymer is of the B-DNA type, with approximately 10 base pairs per turn and a pitch of 33 Å (Fig. 7). It differs from the classical DNA structure in having an alternating, sequence-dependent conformation and hence a dinucleotide repeat unit. In the present model, the A-T overlap is larger, whereas the T-A overlap is smaller than that of B-DNA.[22] Such a poor T-A overlap may account for the observed break of the helical direction from T to A in the crystal structure. The intermolecular adenine–adenine and ribose–thymine interactions (Fig. 5) that are allowed by this break more than compensate for the loss of intramolecular T-A stacking energy. The model embodies the alternating sugar conformation found in the crystal structure and also shows a difference in phosphate diester conformation between A-T and T-A sequences ($\omega' \simeq -70°$ between A and T, $\simeq -125°$ between T and A). The helical turn per base pair is also different for the two sequences: 31° between A and T and 41° between T and A.

Such a sequence-dependent variation in the local conformation of the deoxyribose–phosphodiester backbone may account for the observations that (A·T)-rich regions of DNA and poly(dA-dT) differ in several biochemical and physicochemical properties from regions with other sequences.[23–27] An interpretation of these observations in terms of the alternating DNA model has been given elsewhere.[27,28]

More recent physicochemical evidence regarding the alternating nature of the phosphodiester backbone of poly(dA-dT) comes from P^{31}-nmr studies of the highly homogeneous 145 base-pair fragment and a joint x-ray/nmr study on fibers of double-helical poly(dA-dT).[29,30] Alternating structures have been demonstrated for synthetic DNAs in high-salt solution by nmr studies.[31]

Stereochemistry at the Replicating Fork

The classical autoradiography experiments of Cairns[32] have shown that DNA duplicates by forming a fork. The two chains of the parent duplex become separated at the fork and pair with newly made complementary chains. Replication is a complex, multistep process, involving a relatively large number of proteins.[33] The crystal conformation observed here may,

TABLE V
Coordinates (Å) of the Minihelix in Molecular Inertial System

Atom	x	y	z
P4	8.595	−1.385	−1.278
O1P4	8.414	−0.097	−2.065
O2P4	9.787	−2.216	−1.418
O3P4	8.44	−1.169	0.239
O5P4	7.357	−2.241	−1.609
P3	9.221	3.713	0.59
O1P3	8.429	4.272	−0.331
O2P3	10.605	3.34	0.205
O3P3	9.251	4.559	1.876
O5P3	8.408	2.504	1.056
O1R4	4.712	−3.261	−0.831
C1R4	3.946	−3.019	−2.028
C2R4	4.677	−3.126	−3.2
C3R4	5.673	−4.273	−2.808
O3R4	4.962	−5.646	−3.098
C4R4	5.731	−4.055	−1.288
C5R4	7.165	−3.476	−1.005
O1R3	7.039	0.645	2.883
C1R3	5.782	0.007	2.578
C2R3	6.223	−0.851	1.397
C3R3	7.478	−0.268	0.803
C4R3	8.085	0.332	2.126
C5R3	9.084	1.495	1.984
N1T4	3.524	−1.568	−1.728
C2T4	2.054	−1.283	−1.63
O2T4	1.273	−2.234	−1.665
N3T4	1.786	0.021	−1.543
C4T4	2.638	1.085	−1.539
O4T4	2.087	2.134	−1.412
C5T4	4.018	0.721	−1.635
C6T4	4.361	−0.546	−1.817
C7T4	5.055	1.892	−1.582
N1A3	0.857	0.535	1.655
C2A3	1.605	−0.52	1.749
N3A3	3.010	−0.519	1.993
C4A3	3.596	0.666	2.022
C5A3	3.03	1.894	1.804
C6A3	1.415	1.791	1.762
N6A3	0.748	3.014	1.552
N7A3	3.880	2.984	1.932
C8A3	4.859	2.262	2.181
N9A3	4.827	0.989	2.153
P2	−8.645	−1.327	1.397
O1P2	−9.941	−2.056	1.613
O2P2	−8.461	−0.066	2.124
O3P2	−8.639	−1.109	−0.149
O5P2	−7.353	−2.185	1.724
P1	−8.462	3.955	−0.811
O1P1	−7.598	4.453	0.231
O2P1	−9.860	4.206	−0.607
O5P1	−8.142	2.447	−0.999

(*continued*)

TABLE V (*continued*)

Atom	*x*	*y*	*z*
O3P1	−7.896	4.686	−2.207
O1R2	−4.873	−3.131	1.029
C1R2	−3.984	−2.65	2.155
C2R2	−4.764	−2.862	3.264
C3R2	−5.597	−4.129	3.009
O3R2	−4.887	−5.319	3.31
C4R2	−5.755	−4.03	1.651
C5R2	−7.272	−3.609	1.191
O1R1	−7.181	0.552	−2.926
C1R1	−5.947	−0.257	−2.566
C2R1	−6.458	−1.1	−1.375
C3R1	−7.681	−0.341	−0.826
C4R1	−8.3	0.259	−1.948
C5R1	−8.921	1.573	−1.786
N1T2	−3.587	−1.342	1.796
C2T2	−2.254	−1.072	1.562
O2T2	−1.408	−1.965	1.641
N3T2	−1.910	0.228	1.393
C4T2	−2.917	1.292	1.452
O4T2	−2.249	2.381	1.385
C5T2	−4.177	0.918	1.563
C6T2	−4.501	−0.318	1.747
C7T2	−5.212	2.007	1.584
N1A1	−1.026	0.368	−1.682
C2A1	−1.769	−0.736	−1.866
N3A1	−3.139	−0.753	−1.96
C4A1	−3.557	0.496	−2.091
C5A1	−3.069	1.654	−2.033
C6A1	−1.590	1.596	−1.736
N6A1	−0.875	2.608	−1.645
N7A1	−3.859	2.642	−2.062
C8A1	−5.019	2.156	−2.268
N9A1	−4.952	0.775	−2.306

however, provide a possible model for the spatial relationship between the parent and daughter stems at the fork at a particular stage of the replication process.

The model (shown in Fig. 8) is obtained by extending three minihelices that are adjacent to each other in the crystal structure (enclosed within dotted lines in the schematic diagram). All the stereochemical properties found for the tetranucleotide molecules are retained. **P** represents the phosphodiester bridging the parent and daughter duplex, ω' and ω represent the torsion angles about the in-chain P-O3′ and P-O5′ bonds. These values are 168° and −74°, which are the same as those observed in the crystal structure. They correspond to the *trans–gauche* (tg^-) conformation for the bridging phosphodiester. This conformation produces an extended structure for the parent DNA chains at the fork unlike the *gauche–gauche* (g^-g^-) conformation of the backbone within the helical

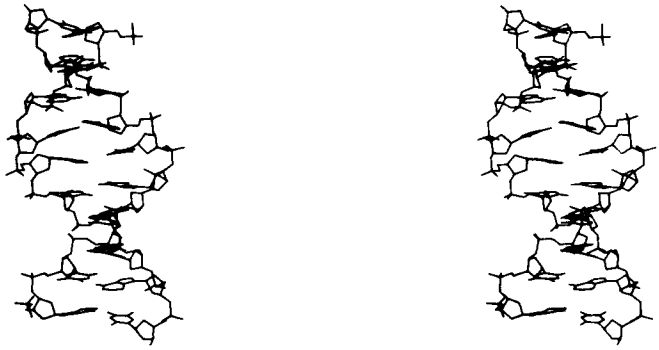

Fig. 7. Computer model of the alternating B-DNA structure obtained by the extension of the minihelix found in the crystal structure.

segments. It also separates adjacent bases on either side of the bridge in each strand by about 14 Å, such that the displaced base can pair satisfactorily with a complementary base of the daughter strand. The base pairs adjacent to the phosphodiester bridging **P** are at almost the same level, whereas the separation within the duplex region is 3.4 Å. The distance between the daughter helix axes is about 23 Å, and the angle subtended on the parent helix axis (angle between planes passing through helix axes) is 120°C. These values are estimated from our model studies, and small changes can be envisaged. It may be noted here that a tg^- phosphodiester conformation has been proposed by Sundaralingam et al.[34] for the messenger RNA during its interaction with the two transfer RNAs.

Several other conformations are possible for the fork depending on the constraints placed on the bridging regions of the backbone. The backbone unit of the polynucleotide chain is composed of six skeletal bonds P-O5′,

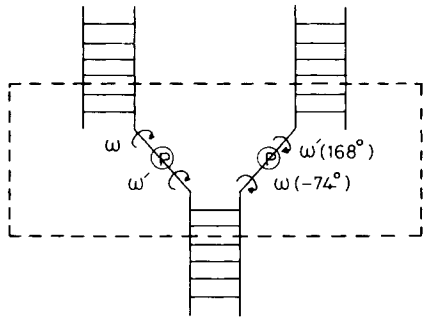

Fig. 8. Stereochemical model of the replication fork, obtained by extending three minihelices found adjacent to each other in the crystal structure (enclosed within dotted line in the schematic diagram). P represents the parent DNA phosphodiester bridging the adjacent nucleotides in the fork region. ω' and ω are torsions around P-O3′ and P-O5′ bonds, respectively. The backbone conformation is tg^- and extended at the fork unlike the g^-g^- conformation within the helical limbs.

O5′-C5′, C5′-C4′, C4′-C3′, C3′-O3′, and O3′-P. The possibility of rotations about these bonds can result in a large number of spatial relationships among the three DNA limbs at the fork region. Earlier analysis of conformational principles in nucleic acids by Sundaralingam[34,35] suggests that the flexibility of polynucleotide chains can be regarded mainly in terms of rotations about the bonds linking successive nucleotide units. A large number of conformational possibilities exist even if rotations about the P-O linkages alone are considered. The present model shows one such possibility and has the attraction that by a change of one single rotation (about P-O3′ of the bridging phosphate) one can bring the three DNA stems at the fork in a satisfactory and close proximity.

We thank the Medical Research Council for financial support and for a Visiting Professorship (to M.A.V.). We are grateful to the D.S.T. and I.C.M.R. (India) for financial support and to SRC for provision of the diffractometer. All crystallographic programs, other than MULTAN, were written by G.M.S. The PLUTO program (unpublished) was provided by Dr. W. D. S. Motherwell.

References

1. Watson, J. D. & Crick, F. H. C. (1953) *Nature* **171,** 737.
2. Arnott, S. (1977) in *Structure and Properties of Biopolymers, Proceedings of the First Cleveland Symposium on Macromolecules*, Walton, A. G., Ed., Elsevier, Amsterdam, 1977.
3. Viswamitra, M. A., Kennard, O., Jones, P. G., Sheldrick, G. M., Salisbury, S., Falvello, L. & Shakked, Z. (1978) *Nature* **273,** 687–688.
4. Wang, A. H.-J., Quingley, G. J., Kolpak, F. J., Crawford, J. L., van Boom, J. H., van der Marel, G. & Rich, A. (1979) *Nature* **282,** 680–686.
5. Drew, H., Takano, T., Tanaka, S., Itakura, K. & Dickerson, R. E. (1980) *Nature* **236,** 567–573.
6. Crawford, J. L., Kolpak, F. J., Wang, A. H.-J., Quigley, G. J., van Boom, J. H., van der Marel, G. & Rich, A. (1980) *Proc. Natl. Acad. Sci. USA* **77,** 4016–4020.
7. Wing, R., Drew, H., Takano, T., Broka, C., Tanaka, S., Itakura, K. & Dickerson, R. E. (1980) *Nature* **287,** 755–758.
8. Weimann, G., Schaller, H. & Khorana, H. G. (1963) *J. Am. Chem. Soc.* **85,** 3835–3840.
9. Main, P., Woolfson, M. M., Lessinger, L., Germain, G. & Declercq, J.-P. (1974) MULTAN, *A System of Computer Programs for the Automatic Solution of Crystal Structures from X-Ray Diffraction Data*, University of York, England.
10. Seeman, N. C., Rosenberg, J. M., Suddath, F. L., Kim, J. J. P. & Rich, A. (1976) *J. Mol. Biol.* **104,** 109–144.
11. Rosenberg, J. M., Seeman, N. C., Day, R. O. & Rich, A. (1976) *J, Mol. Biol.* **104,** 145–167.
12. Hingerty, B., Subramanian, E., Stellman, S. D., Sato, T., Broyde, S. B. & Langridge, R. (1976) *Acta Crystallogr., Sect. B* **32,** 2998–3013.
13. Karle, J. (1968) *Acta Crystallogr., Sect. B* **24,** 182–186.
14. Levitt, M. (1978) *Proc. Natl. Acad. Sci. USA* **75,** 640–644.
15. Sundaralingam, M. (1969) *Biopolymers* **7,** 821–860.
16. Viswamitra, M. A., Reddy, B. S., Lin, G. H. & Sundaralingam, M. (1971) *J. Am. Chem. Soc.* **93,** 4565–4573.
17. Sussman, J. L., Seeman, N. C., Kim, S. H. & Berman, H. M. (1972) *J. Mol. Biol.* **66,** 403–421.
18. Rubin, J., Brenner, T. & Sundaralingam, M. (1972) *Biochemistry* **11,** 3112–3228.
19. Camerman, N., Fawcett, J. K. & Camerman, A. (1976) *J. Mol. Biol.* **107,** 601–621.

20. Motherwell, W. D. S. & Isaacs, N. W. (1972) *J. Mol. Biol.* **71,** 231–241.
21. Jack, A. (1977) *Acta Crystallogr., Sect. A* **33,** 497–499.
22. Arnott, S., Chandrasekaran, R., Hukins, D. W. L., Smith, P. J. C. & Watts, L. (1974) *J. Mol. Biol.* **88,** 523–533.
23. Bram, S. (1971) *Nature [New Biol.]* **232,** 174–176.
24. Johnson, P. H. & Laskowski, M. S. (1970) *J. Biol. Chem.* **245,** 891–898.
25. Scheffler, I. E., Elson, E. L. & Baldwin, R. L. (1968) *J. Mol. Biol.* **36,** 291–304.
26. Richmond, T. & Steitz, T. A. (1976) *J. Mol.Biol.* **103,** 25–38.
27. Viswamitra, M. A., Kennard, O., Shakked, Z., Jones, P. G., Sheldrick, G. M., Salisbury, S. & Falvello, L. (1978) *Curr. Sci.* **9,** 289–292.
28. Klug, A., Jack, A., Viswamitra, M. A., Kennard, O., Shakked, Z. & Steitz, T. A. (1979) *J. Mol. Biol.* **131,** 669–680.
29. Shindo, H., Simpson, R. T. & Cohen, J. S. (1979) *J. Biol. Chem.* **254,** 8125–8128.
30. Shindo, H. & Zimmerman, S. B. (1980) *Nature* **283,** 690–691.
31. Patel, D. J. (1980) in *Abstracts of Nucleic Acids: Interactions with Drugs and Carcinogens*, British Biophysical Society Meeting, London.
32. Cairns J. (1963) *J. Mol. Biol.* **6,** 208–213.
33. Alberts, B. & Sternglanz, R. (1977) *Nature* **269,** 655–661, and references cited therein.
34. Sundaralingam, M., Brennan, T., Yathindra, N. & Ichikawa, T. (1975) in *Structure and Conformation of Nucleic Acids and Protein-Nucleic Acid Interaction*, Sundaralingam, M. & Rao, S. T., Eds., University Park Press, Baltimore, pp. 101–113.
35. Sundaralingam, M. (1973) *Int. J. Quantum Chem., Quantum Biol.* **1,** 81–91.

Received April 22, 1981
Accepted July 29, 1981